

# Simulations of the response of mesospheric circulation and temperature to the Antarctic ozone hole

Anne K. Smith,<sup>1</sup> Rolando R. Garcia,<sup>1</sup> Daniel R. Marsh,<sup>1</sup> Douglas E. Kinnison,<sup>1</sup> and Jadwiga H. Richter<sup>2</sup>

Received 24 August 2010; revised 20 September 2010; accepted 28 September 2010; published 18 November 2010.

[1] The loss of ozone that has occurred in the Antarctic lower stratosphere during each spring since 1980 has led to a decrease in the lower stratospheric temperature that persists into the summer season. The temperature changes are accompanied by changes in the zonal wind in the SH stratosphere that affect the filtering of gravity waves propagating into the mesosphere. In simulations with the Whole Atmosphere Community Climate Model (WACCM), the resulting gravity wave changes have led to a weakening of the SH summer upwelling around 65–80 km and of the equatorward flow around 0.01 hPa. The trend occurs primarily in the years 1975–1990. The circulation changes are accompanied by an increase in the SH temperature at 65–85 km and a decrease at 95 km. Comparison of the summer temperatures in the NH and SH indicates a distinctive offset beginning around 1980. The increase in temperature near the SH summer mesopause has implications for the presence of polar mesospheric clouds. **Citation:** Smith, A. K., R. R. Garcia, D. R. Marsh, D. E. Kinnison, and J. H. Richter (2010), Simulations of the response of mesospheric circulation and temperature to the Antarctic ozone hole, *Geophys. Res. Lett.*, 37, L22803, doi:10.1029/2010GL045255.

## 1. Introduction

[2] Observations indicate hemispheric asymmetries in the altitude and brightness of polar mesospheric clouds (PMC) and in the altitude and temperature of the polar mesopause. PMC occur less frequently in the SH and their mean altitude is higher [Bailey *et al.*, 2007]. The altitude of the mesopause is higher and warmer in the SH summer [e.g., Xu *et al.*, 2007]. Mechanisms that have been proposed to explain the differences draw on radiative (Earth-Sun distance) or dynamical (gravity wave forcing) processes. In this study, we show that dynamical processes associated with the ozone hole in the Antarctic stratosphere could contribute to these hemispheric differences.

[3] The Antarctic ozone hole is characterized by extensive destruction of lower stratospheric ozone across the polar vortex region during the southern spring. The extent of the loss varies somewhat from year to year but has been present for every year since 1980 [World Meteorological Organization, 2007; Solomon *et al.*, 2005]. The loss of ozone leads to a reduction in the heating by absorption of

solar radiation. The resulting negative trend in temperature [Thompson and Solomon, 2002; Randel *et al.*, 2009] is largest during the months October–December over the pressure range 300–50 hPa. There are also changes to the geopotential height that affect the zonal wind in the troposphere and stratosphere [Gillett and Thompson, 2003]. The trends are simulated in chemical climate models that include stratospheric chemistry [e.g., Eyring *et al.*, 2006; *Stratospheric Processes and Their Role in Climate* (SPARC), 2010].

[4] Strong gravity wave (GW) breaking and dissipation in the mesosphere leads to momentum flux divergence that drives a vigorous summer to winter circulation. The propagation of GW from the troposphere into the mesosphere depends on the wind distribution in the intervening atmosphere, including the stratosphere [Holton, 1983]. Therefore, a change in the SH stratospheric zonal jet associated with the Antarctic ozone loss can have an impact on the GW spectrum that is able to propagate into the mesosphere [Manzini *et al.*, 2003].

[5] The factors just described give a scenario for the ozone hole to affect the mesospheric circulation and temperature. The stratospheric wind changes associated with the ozone loss affect the propagation of GW that drive the circulation in the mesosphere. That circulation is characterized by strong upwelling that is responsible for the extremely cold temperatures found at the summer polar mesopause. When the strength of the upwelling weakens, the adiabatic cooling decreases and therefore the temperature increases.

## 2. Description of Model and Analysis

[6] The Whole Atmosphere Community Climate Model (WACCM) is a high-top model based on the NCAR Community Climate System Model. The atmospheric component of WACCM extends from the Earth's surface to  $5.96 \times 10^{-6}$  hPa and includes interactive chemistry, radiation, and dynamics. We use WACCM version 3.5, which uses the physics suite from CAM3.5. Garcia *et al.* [2007] give a detailed description of an earlier version of WACCM and Richter *et al.* [2010] give updates. The present integrations have longitude and latitude resolution of  $2.5^\circ$  and  $1.9^\circ$ ; vertical resolution is about 1.25 km in the lower stratosphere, decreases to 1.75 km in the upper stratosphere, and 3.5 km above 65 km. WACCM includes a parameterization of the effects of GW on the winds and circulation described by Richter *et al.* [2010]. Note particularly that the GW sources in the troposphere are not fixed but instead respond to changing climate conditions.

[7] Four WACCM integrations beginning in 1953 and extending through 2006 were performed as part of the

<sup>1</sup>Atmospheric Chemistry Division, National Center for Atmospheric Research, Boulder, Colorado, USA.

<sup>2</sup>Chemistry and Global Dynamics, National Center for Atmospheric Research, Boulder, Colorado, USA.

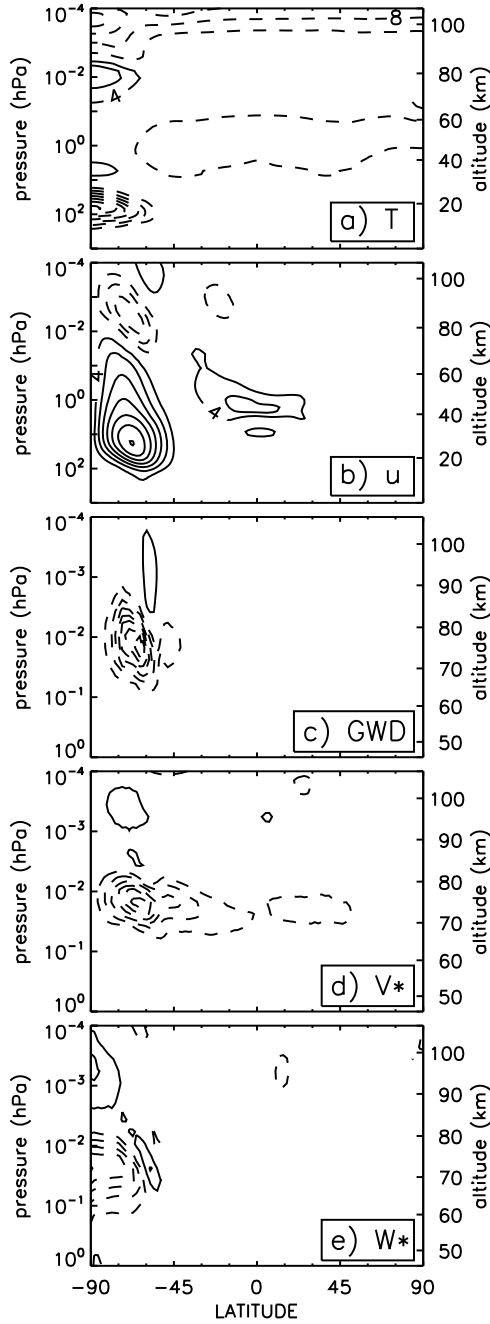


**Figure 1.** Linear trends in (a) temperature (units: K/47 years; contour intervals 4), (b) zonal wind (units: m/s/47 years; contour intervals 4), (c) gravity wave drag (units: m/s/day/47 years; contour intervals 8), (d)  $\bar{v}^*$  (units: m/s/47 years; contour intervals 0.4), and (e)  $\bar{w}^*$  (units: cm/s/47 years; contour intervals 0.2) over the period 1960–2006 averaged over the months of November and December and over four realizations of WACCM. Negative contours are dashed and zero contours are not drawn. The vertical range differs between frames.

REF-B1 activities for the CCMVal project of SPARC (Stratospheric Processes and their Role in Climate); see SPARC [2010] and Morgenstern *et al.* [2010] for descriptions of this model comparison project. These integrations follow the REF-B1 forcing scenario in which model values

for sea surface temperatures, anthropogenic and natural surface gas abundances, solar flux, geomagnetic activity, volcanic aerosols, and the momentum forcing needed to produce a realistic parameterized QBO were specified from observations. With slight differences in the initial conditions, the four different runs produce different realizations of the same climate, such that there may be substantial differences among them in any given calendar month or year. Monthly mean output from these four integrations for the period 1960 through 2006 are analyzed here. We also show results from an additional “fixed halogen” run in which the surface abundances of halogen compounds are held fixed at 1960 levels. The increase in chlorofluorocarbon emissions that occurred after 1960 is not included and, as a consequence, no Antarctic ozone hole develops.

[8] Middle atmosphere responses to the 11-year solar cycle, to the quasi-biennial oscillation (QBO) in tropical zonal wind, and to the variations in volcanic aerosols can mask trends from other sources. The usual approach, also adopted here, is to use linear multiple regression to account simultaneously for these effects. For the large and highly significant trends presented here, there is virtually no difference in the trends determined by the regression analysis and a trend determined from a linear least-squares fit to the time series. We calculate the trend for individual months over the period 1960–2006 using a linear multiple regression fit with five terms: a linear trend, the 11-year solar cycle, two orthogonal QBO terms, and a volcanic aerosol index. The four model runs are analyzed separately so we end up with four estimates of the trend.

### 3. Trends

[9] Figure 1 shows the trends in zonally averaged temperature, zonal wind, GW drag, transformed Eulerian mean (TEM) meridional velocity ( $\bar{v}^*$ ) and TEM vertical velocity ( $\bar{w}^*$ ) averaged for November and December. The TEM circulation [Andrews and McIntyre, 1976] is an Eulerian representation of the zonally averaged Lagrangian motion due to the mean and perturbation winds. Trend results from the four model cases have been averaged together but the trends in SH high latitudes are also seen very strongly in each individual integration and in either of these two months treated separately.

[10] The negative temperature trend in the SH polar lower stratosphere is a result of ozone loss. The annual destruction of ozone occurs in the spring when sunlight activates the catalytic cycles that allow chlorine and bromine to rapidly deplete ozone. The ozone concentrations in the model typically recover by January [SPARC, 2010]. The early summer stratospheric temperature trend in WACCM is larger than observed by about a factor of two, probably because the ozone recovery is delayed in the model relative to the observed timing. The magnitudes of the simulated mesospheric trends may be exaggerated as well although we do not have sufficient observations from the 1970s to verify this.

[11] Through the thermal wind relation, the negative trend in stratospheric polar temperature is related to a positive trend in zonal wind that has a maximum around 20–30 hPa and 60–70°S. The stratospheric zonal wind during November and December is in transition from the wintertime westerly winds to the summertime easterlies. Since the

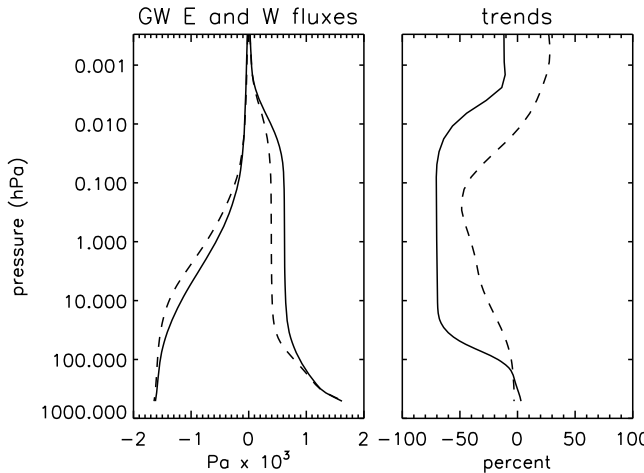


**Figure 2.** (left) Average GW eastward (positive) and westward (negative) momentum fluxes from years prior to the onset of polar ozone loss (1960–1975; solid lines) and afterwards (1985–2006; dashed lines) for latitudes 60°–75°S. (right) Percent trends between 1960 and 2006 of the eastward (solid) and westward (dashed) fluxes.

onset of the ozone hole, the timing of that transition in the model is delayed relative to its occurrence in the 1960s and 1970s and also relative to the comparable transition in the NH. The positive SH trend during early summer is a result of the persistence in the westerly flow in the lower stratosphere. The delay in the winter to summer transition leads to further delay in the ozone recovery; the ozone trend and circulation changes are interactive and cannot be readily isolated.

[12] The change in zonal wind increases the filtering of eastward GW and reduces the magnitude of the eastward momentum forcing when the waves dissipate in the mesosphere. The impact on  $\bar{v}^*$  is a reduction of the equatorward flow that is strongest at 0.01 hPa.  $\bar{w}^*$  has a negative trend centered at 0.03 hPa (weaker upwelling for the upwelling part of the circulation) and a positive trend centered at 0.0003 (weaker downwelling for the downwelling part of the circulation). Adiabatic effects lead to positive and negative temperature trends at 0.03 and 0.0003 hPa, respectively. The comparable trends for May–June in the NH (not shown) are very small and are inconsistent between the four realizations of the models.

[13] In the WACCM parameterization of GW drag [Richter *et al.*, 2010], a spectrum of waves is launched at 600 hPa when a criterion determining the presence of a front is met. Trends in GW drag can result from changes in the filtering of the waves by stratospheric winds or changes in the wave sources in the troposphere. Analysis of the trends in the upward wave momentum fluxes in the SH are shown in Figure 2. There are very small changes (~2% increase) at the wave source region near 600 hPa. Clearly, trends in the GW sources used by the parameterization do not make an important contribution to the trends in the GW drag in the mesosphere. In comparison, in the lower stratosphere there are appreciable trends in the eastward and westward stresses: the eastward stress decreases in magnitude by 73% while the westward stress increases in magnitude and becomes more strongly westward. The net effect is to weaken

the normally eastward net GW drag at the altitude where the waves break in the mesosphere (Figure 1).

[14] Figure 3 shows time series of temperature and ozone mixing ratio at high latitudes during December in the SH and June in the NH. The temperature sequences highlight the differences in the temperature behavior in the two hemispheres. At 72 and 0.01 hPa, summer temperatures in the two hemispheres are much closer to one another prior to about 1977 and then diverge in concert with the stratospheric ozone loss. At 0.0003 hPa (~98 km), the opposite occurs; the SH summer temperature is initially warmer but, around 1980, cools and is similar to that in the NH summer thereafter.

[15] Figure 3 also includes time series from the “fixed halogen” run. In this case ozone loss due to anthropogenic gases is strongly reduced and no ozone hole develops. The differences between the fixed halogen case and the ensemble average of the normal runs confirms that it is indeed the stratospheric ozone loss that is responsible for the changing relationship between summer temperatures in the two hemispheres, even in the MLT region.

[16] There are only slight differences in the NH polar temperature at the mesopause (0.004 hPa; ~84 km) before and after the onset of the ozone hole (Figure 4). However, in the SH the temperature of the mesopause has warmed by 4.6K whereas the SH temperature near 0.001 hPa has cooled

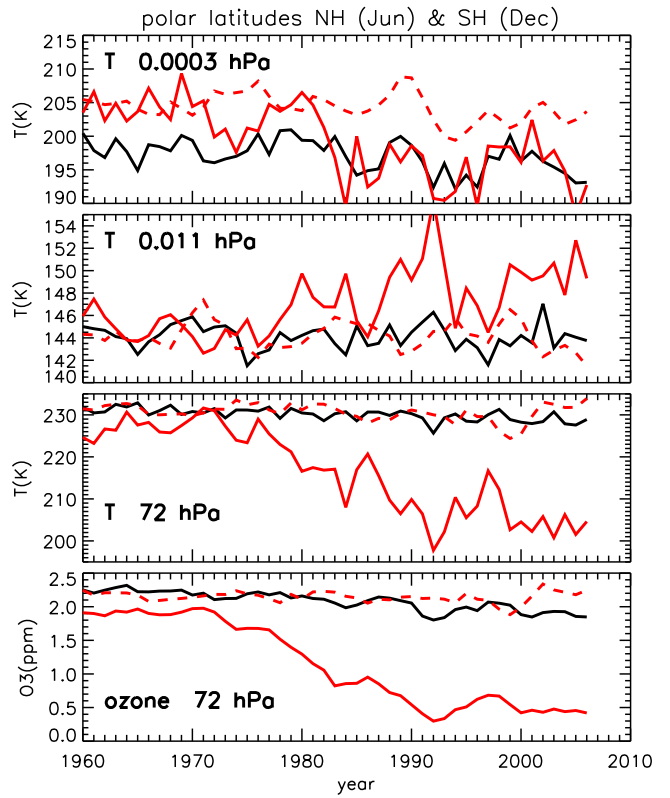


**Figure 3.** Time series of temperature at three levels in the middle atmosphere and ozone in the lower stratosphere. Solid curves are averages from four WACCM realizations; red for December at 80–90°S (SH summer) and black for June at 80–90°N (NH summer). The red dashed line are averages for December at 80–90°S from a model run in which the emissions of halogen compounds were held fixed at their 1960 levels.

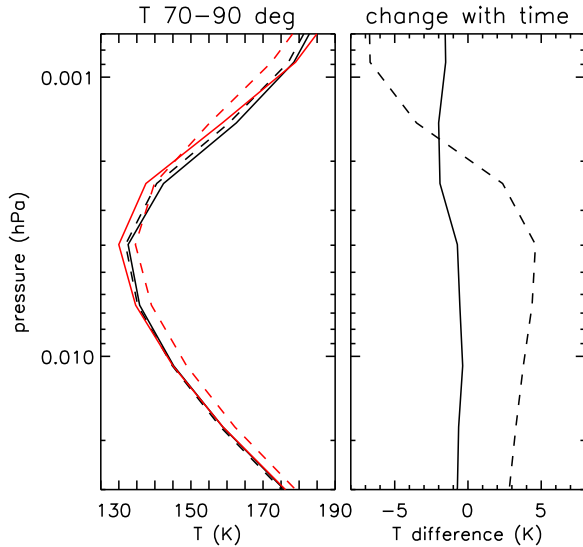


**Figure 4.** (left) Average temperature profiles from years prior to the onset of polar ozone loss (1960–1975; solid lines) and afterwards (1985–2006; dashed lines); black: June averages for 80–90°N; red: December averages for 80–90°S. (right) Difference between the two periods for the NH (solid) and SH (dashed).

by more than 6K. No shifts in the pressure of the temperature minimum are apparent with the current model resolution. The SH temperature change is sufficient to reverse the sign of the mesopause temperature asymmetry. Prior to 1975, the SH summer mesopause was colder than that in the NH; since 1985, it has been warmer. PMCs are found in the summer polar region at altitudes near and just below the mesopause where the temperature is very cold. The temperature trends described here imply that the conditions in the SH have become less favorable for the existence of these clouds. This again is consistent with observations showing that the frequency of occurrence of the clouds is lower in the SH than in the NH [Bailey *et al.*, 2007].

#### 4. Conclusions

[17] We used NCAR's Whole Atmosphere Community Climate Model to investigate the trends in the upper mesosphere circulation and temperature. The results indicate that there is a strong trend over the period 1960–2006 in the strength of the GW driven circulation in high southern latitudes during late spring and early summer that is largest during November and December. The accompanying temperature trend is positive at 0.01 hPa and negative at 0.0001 hPa.

[18] The mechanism for the trend in WACCM is straightforward. Cooling has occurred in the lower stratosphere due to the strong reduction of ozone in the SH spring and early summer known as the Antarctic ozone hole. The increase in the positive temperature gradient is associated with the persistence of westerly winds longer into early summer in the lower stratosphere. The SH temperature trends simulated by WACCM are similar in morphology but larger in amplitude by about a factor of two compared to those seen in observations [Thompson and Solomon, 2002; Randel *et al.*, 2009].

[19] The GW that drive the strong summer to winter flow in the mesosphere are filtered by stratospheric winds. The strengthening of the stratospheric early summer westerly jet since 1980 has led to a weaker net GW forcing in the mesosphere, which is directly responsible for the weakening of the mean circulation. The decreases in the upwelling around 0.01 hPa and the downwelling around 0.0001 hPa at the SH summer pole affect the temperature through reductions in the adiabatic cooling and heating; this accounts for the trends in the temperature in these regions.

[20] Comparisons between the temperatures in the NH and SH indicate that they are more similar in the early part of the integration, before the onset of the ozone hole around 1980. The temperature increases at 0.01 hPa in the SH, without a comparable strong change in the NH, contributed to an offset in the temperature changes between the hemispheres. Hemispheric differences in temperature [Xu *et al.*, 2007] and polar mesospheric cloud occurrence frequencies [Bailey *et al.*, 2007] have been reported for current-day conditions and are consistent with the WACCM simulations.

[21] The Antarctic ozone hole is perhaps the largest persistent perturbations to the atmosphere during recent decades. As shown here, the climate impacts of this anthropogenic change extend into the upper mesosphere. As the ozone recovers in upcoming decades, we expect to see shifts in the SH summer mesopause that bring it closer to that in the NH.

[22] **Acknowledgments.** The National Center for Atmospheric Research is sponsored by the National Science Foundation. Support for this work was also provided by the NASA Heliospheric Guest Investigator Program.

#### References

Andrews, D. G., and M. E. McIntyre (1976), Planetary waves in horizontal and vertical shear: The generalized Eliassen-Palm relation and the zonal mean acceleration, *J. Atmos. Sci.*, 33, 2031–2048.

Bailey, S. M., A. W. Merkel, G. E. Thomas, and D. W. Rusch (2007), Hemispheric differences in polar mesospheric cloud morphology observed by the Student Nitric Oxide Explorer, *J. Atmos. Sol. Terr. Phys.*, 69, 1407–1418.

Eyring, V., et al. (2006), Assessment of temperature, trace species, and ozone in chemistry-climate model simulations of the recent past, *J. Geophys. Res.*, 111, D22308, doi:10.1029/2006JD007327.

Garcia, R. R., D. R. Marsh, D. E. Kinnison, B. A. Boville, and F. Sassi (2007), Simulation of secular trends in the middle atmosphere, 1950–2003, *J. Geophys. Res.*, 112, D09301, doi:10.1029/2006JD007485.

Gillett, N. P., and D. W. J. Thompson (2003), Simulation of recent Southern Hemisphere climate change, *Science*, 302, 273–275, doi:10.1126/science.1087440.

Holton, J. R. (1983), The influence of gravity wave breaking on the general circulation of the middle atmosphere, *J. Atmos. Sci.*, 40, 2497–2507.

Manzini, E., B. Steil, C. Brühl, M. A. Giorgetta, and K. Krüger (2003), A new interactive chemistry-climate model: 2. Sensitivity of the middle atmosphere to ozone depletion and increase in greenhouse gases and implications for recent stratospheric cooling, *J. Geophys. Res.*, 108(D14), 4429, doi:10.1029/2002JD002977.

Morgenstern, O., et al. (2010), Review of the formulation of present-generation stratospheric chemistry-climate models and associated external forcings, *J. Geophys. Res.*, 115, D00M02, doi:10.1029/2009JD013728.

Randel, W. J., et al. (2009), An update of observed stratospheric temperature trends, *J. Geophys. Res.*, 114, D02107, doi:10.1029/2008JD010421.

Richter, J. H., F. Sassi, and R. R. Garcia (2010), Towards a physically based gravity wave source parameterization in a general circulation model, *J. Atmos. Sci.*, 67, 136–156.

Solomon, S., R. W. Portmann, T. Sasaki, D. J. Hofmann, and D. W. J. Thompson (2005), Four decades of ozonesonde measurements over Antarctica, *J. Geophys. Res.*, 110, D21311, doi:10.1029/2005JD005917.

Stratospheric Processes and Their Role in Climate (SPARC) (2010), *Report on the Evaluation of Chemistry-Climate Models*, edited by V. Eyring, T. G. Shepherd, and D. W. Waugh, *SPARC Rep.* 4, World Meteorol.

Organ, Geneva, Switzerland. (Available at <http://www.atmosp.physics.utoronto.ca/SPARC>)

Thompson, D. W. J., and S. Solomon (2002), Interpretation of recent Southern Hemisphere climate change, *Science*, 296, 895–899, doi:10.1126/science.1069270.

World Meteorological Organization (2007), Scientific Assessment of Ozone Depletion: 2006, *Global Ozone Res. Monit. Proj. Rep.* 50, 572 pp., Geneva, Switzerland.

Xu, J., H.-L. Liu, W. Yuan, A. K. Smith, R. G. Roble, C. J. Mertens, J. M. Russell III, and M. G. Mlynczak (2007), Mesopause structure from Thermosphere, Ionosphere, Mesosphere, Energetics, and Dynamics (TIMED)/Sounding of the Atmosphere Using Broadband Emission Radiometry (SABER) observations, *J. Geophys. Res.*, 112, D09102, doi:10.1029/2006JD007711.

---

R. R. Garcia, D. E. Kinnison, D. R. Marsh, and A. K. Smith, Atmospheric Chemistry Division, National Center for Atmospheric Research, PO Box 3000, Boulder, CO 80307, USA. (aksmith@ucar.edu)

J. H. Richter, Chemistry and Global Dynamics, National Center for Atmospheric Research, PO Box 3000, Boulder, CO 80307, USA.